

**EVALUATION OF ASR DISTRESS IN AIRFIELD CONCRETE PAVEMENTS**

By:

Seungwook Lim, Dan G. Zollinger, Ph.D., P.E. and Shondeep L. Sarkar, Ph.D., P.E.  
Texas Transportation Institute, Texas A&M University  
College Station, TX 77843-3135

PRESENTED FOR THE 2002 FEDERAL AVIATION ADMINISTRATION AIRPORT  
TECHNOLOGY TRANSFER CONFERENCE

05/02

## **ABSTRACT**

This paper focuses on the development of a framework for evaluation of ASR-induced damage in airfield concrete pavements. A US airport was selected for this purpose. The framework consisted of visual inspection, in-field detection of ASR gel, and laboratory investigations. The study indicates that proper in-field detection of ASR gel can significantly reduce cost and evaluation time. Using uranyl acetate solution as a diagnostic tool for detection of ASR holds promise as a field kit. However, by itself it does not serve as a decision making tool. Laboratory investigation of core samples is recommended for verification of ASR and for assessment of extent of damage.

## **INTRODUCTION**

ASR in concrete is an expansive reaction phenomenon, which causes concrete to crack, and may eventually compromise the integrity of the structure. Airfield concrete pavements are not free of this deleterious reaction. Typical ASR distress manifests as map or pattern cracks, joint misalignments, heaving, and aggregate pop-outs. However, similar features can develop from other distress mechanisms such as freeze-thaw, corrosion of metal reinforcement, and ground movement, and are in fact, hardly distinguishable from visual inspection. Clear identification of ASR and its degree of severity is a crucial prerequisite for taking proper mitigative measures.

One US airport with pre-established symptoms of pavement distress was selected for the purpose of this study. The airport is located in an area of high-altitude (5,000ft), dry environment (precipitation from 0.4 to 1.4 inches) with RH as low as 20%, and temperatures in the range of 35°F and 80°F. The evaluation process consisted of (1) a detailed visual inspection with emphasis on the nature and distribution pattern of cracks, (2) detection of ASR gel in the field using uranyl acetate fluorescent dye, and (3) laboratory analysis of cored samples for verification and proper assessment of ASR damage. This paper discusses the results of the evaluation in two parts, namely, field evaluation and laboratory investigations.

## **FIELD EVALUATION**

Seven different sections of concrete pavements, including runway, taxiway, and apron were selected for a detailed visual inspection. The general descriptions of the test sections are summarized in Table 1. All the test sections showed typical expansive distress features, such as map cracks, compressed joints, and joint misalignments, in different degrees of severity. Figure 1 shows some of the distress features observed. Upheaval of pavements was noted to be minimal in these sections, but joint misalignment was conspicuous. Aggregate pop-outs were also negligible in proportion to the amount of distress.

One unique feature of ASR is the presence of “gel”, a reaction product of ASR. Although not always present on the exposed surface, it helps to identify ASR. In some cases, the gel product can be recognized with unaided eye from exudation on concrete surface. Figure 2 shows an example of gel exudation observed in pavement section 4. It should be noted, however, that this exudation normally indicates severely processed ASR. The pavement shown in Figure 2 was constructed in 1950s, and is no longer in service. In most cases, expert microscopic examination

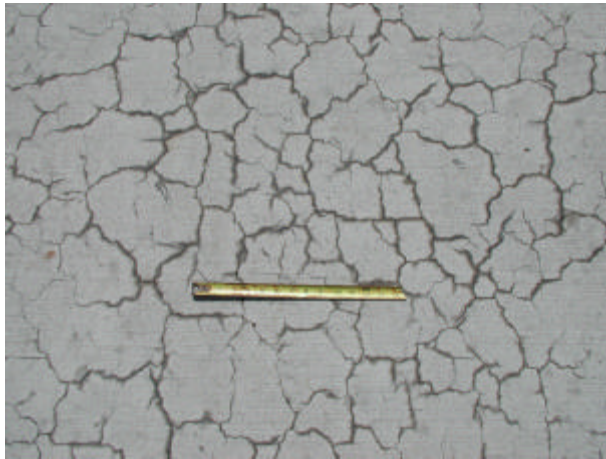
**Table 1.** Brief description of visible distress features in the test sections selected

Section No.	Year Constructed	Visible Distress Features
1	1960's	<ul style="list-style-type: none"> <li>▪ severe map cracks, compressed joints, joint misalignment, faulting</li> <li>▪ slab expansion resulted in structural distortion of columns in neighboring building</li> <li>▪ surface treated with one coat of slurry seal also shows map cracking</li> </ul>
2	1985	<ul style="list-style-type: none"> <li>▪ map cracks of various severity, discrete cracks at joints, compressed joint with minor spalling</li> <li>▪ severe map cracks also manifest in surrounding concrete structures</li> </ul>
3A	1987	<ul style="list-style-type: none"> <li>▪ structural cracks, moderate map cracking, low severity aggregate pop-outs</li> </ul>
3B*	1985	<ul style="list-style-type: none"> <li>▪ lesser number or no cracks compared to section 3A</li> </ul>
4	1950's	<ul style="list-style-type: none"> <li>▪ severe structural cracks, severe map cracks, ASR gel exudation</li> <li>▪ area currently not in service</li> </ul>
5	1945	<ul style="list-style-type: none"> <li>▪ moderate structural cracks, map cracks, and pop-outs</li> <li>▪ area currently not in service</li> </ul>
6	1987	<ul style="list-style-type: none"> <li>▪ slabs and joints in good condition</li> <li>▪ faintly visible map cracks appear when surface is wet</li> </ul>

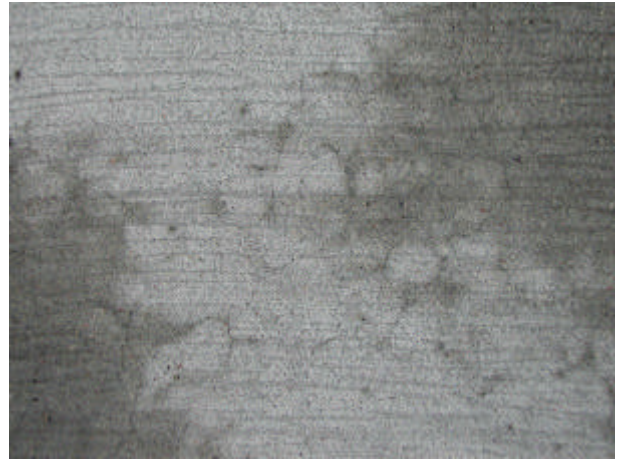
\* Located immediately next to section 3A

in a properly equipped laboratory is required to identify the gel in the early stages of ASR. Effective in-field detection of gel would significantly reduce the time and cost of evaluation process.

A method of in-field detection of ASR gel, called the uranyl acetate fluorescence method (UAFM), was developed with using uranyl acetate solution <sup>(1)</sup>. The gel is essentially composed of silica, alkalis (sodium and/or potassium), and calcium <sup>(2)</sup>. The uranyl ion substitutes for alkali in the gel, generating a characteristic bright yellowish green glow under ultraviolet light. UAFM was used as a part of field evaluation process at three locations showing varying severity of map cracks. First, the pavement surface was lightly chipped to expose fresh concrete surface. The prepared surface was cleaned with distilled water and dried before applying uranyl acetate solution. Three to five minutes was allowed for the applied solution to react with the ASR gel, and then inspected under a closed UV light box. UAFM showed indefinite evidence of ASR gel at all three test sections regardless of the severity of cracking. The characteristic glow was observed only in a limited number of air voids at the test surface.



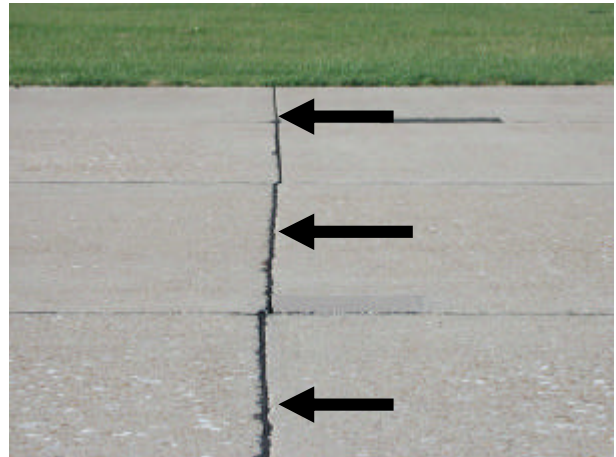
(a) High severity map cracks (section 2)



(b) Low severity map cracks (section 6)



(c) Compressed joint (section 2)



(d) Joint misalignment (section 3A)

**Figure 1.** Typically observed distress features



**Figure 2.** Exudation of ASR gel through cracks

## LABORATORY INVESTIGATIONS

### Visual Inspection of Cores

Concrete cores were collected from each test pavement section for laboratory investigations. General descriptions of these cores are summarized in Table 2. Although the pavement in all the test sections showed various levels of expansive distresses, signs of ASR were observed only in 5 cores. Blight et al. <sup>(3)</sup> used a scoring method to identify ASR based on 5 different visual characteristics of concrete, viz. (1) dark reaction rims around aggregate particles, (2) white acid-insoluble reaction products, (3) cracks in aggregate particles, (4) cracks in paste, and (5) interface cracks between mortar and aggregates. Only the core from section 1 satisfied all these criteria. Cores from sections 2, 3A, 4, and 5 scored 2 to 4 matches.

**Table 2.** Brief description of distress symptoms in cores from test sections

Section No.	Approximate coring location	Distress features
1	Slab center	<ul style="list-style-type: none"> <li>▪ surface cracks propagate vertically to less than 3-inch depth, and below that delamination type cracks prevail throughout the thickness</li> <li>▪ dark reaction rims around aggregate</li> <li>▪ white gel deposit around aggregate, in air voids, and cracks</li> <li>▪ cracks in aggregate, paste, and paste-aggregate interface</li> </ul>
2	3 ft. from joint	<ul style="list-style-type: none"> <li>▪ surface cracks propagate vertically to less than 3" depth, and no visible cracks below that</li> <li>▪ white gel deposits around aggregate, in air voids</li> </ul>
3A	3 ft. from joint	<ul style="list-style-type: none"> <li>▪ surface cracks propagate vertically to less than 3" depth, and no visible cracks below that</li> <li>▪ white gel deposits around aggregate, in air voids</li> </ul>
3B	3 ft. from joint	<ul style="list-style-type: none"> <li>▪ no visible cracks</li> </ul>
4	Slab center	<ul style="list-style-type: none"> <li>▪ structural crack from top surface to bottom</li> <li>▪ white gel deposits around aggregate, in air voids, and cracks</li> <li>▪ cracks in aggregate, paste, and paste-aggregate interface</li> </ul>
5	Slab center	<ul style="list-style-type: none"> <li>▪ cracks propagate vertically less than 3" from surface and bottom. These are connected by hairline cracks in mid-depth area</li> <li>▪ cracks in aggregate, paste, and paste-aggregate interface</li> </ul>
6	2 ft. from joint	<ul style="list-style-type: none"> <li>▪ clean and no visible cracks</li> </ul>

Figure 3 shows some cores taken from the test sections. Cracks of varying severity are visible. Numbers shown in the pictures represent the identification of test section. Test sections 1 and 2 showed severe map cracks, while map cracks in section 6 were faintly visible when the surface was wetted. The condition of test sections 2 and 6 are represented in the Figures 1 (a) and 1 (b), respectively. Figure 3 clearly indicates that concrete cores from sections 1 and 2 that have high severity cracking, manifest more damage compared to the core from section 6, that has low severity cracking.

It is interesting to compare the cores from sections 1 and 2 (Figures 3 (a) and (b)). Both sections manifested high severity map cracking, and crack density shown on the pavement surface was estimated to be the same. However, the cores indicate that the degree of deterioration under the surface is significantly different. This is attributed to the age of the concrete. Pavement section 1 has been in service over 20 years longer than section 2, and presumably so does the period of ASR development.

The difference also helps to explain the mechanism of cracking due to ASR. General sequence of ASR distress follows steps such (a) development of high concentration of alkalis in pore solution, (b) reaction with aggregate and formation of reaction gel product, (c) expansion arising from moisture flow into the gel, and (d) cracking and subsequent deterioration<sup>(4)</sup>. Pore solution near the slab surface generally has high alkali concentration due to drying of pore water, and therefore, the reaction and subsequent gel formation is more preponderant at the surface. Moisture, that is required for the gel to expand, is also easily accessible at pavement surface. As a consequence, ASR deterioration tends to initiate from the surface. Concrete expansion at or near a free surface can result in bursting of the concrete, and subsequent vertical cracking. The cracks provide pathways for pore water evaporation as well as for the ingress of external water into concrete. As a result, deterioration continues to proceed to inner concrete. Although the expansive force should be same in all directions, actual expansion occurs in the direction of least restraint. The confining effect in the direction of the thickness of the slab is much less than in the lateral direction. Furthermore, by then the concrete near the upper surface has already weakened. Therefore, the inner concrete tends to disintegrate upward rather than expand laterally.

Similar cracking mechanism may occur at the bottom of slab as observed on the core from section 5 (Table 2). Moisture is also highly available at the bottom of pavement. Furthermore, water can be entrapped for a long time at the slab-subbase interface depend on subbase material and drainage condition. This continuous moisture supply will accelerate gel expansion and subsequent cracking at the bottom of slab.

### **Application of uranyl acetate fluorescent method**

In addition to field application, the efficacy of UAFM was evaluated on cores in the laboratory. Cores were sliced into two or three pieces as a function of depth, and uranyl acetate solution was applied to the sectional surface of each slice. Figure 4 shows sliced core samples before and after UAFM. The core shown in this figure was collected from section 1. The length of core was 14.5 inches, and it was cut into three pieces at 2, 6, and 12-inch depth. By applying UAFM, the presence of ASR gel is identified by bright yellowish green glow under UV light. UAFM revealed clear evidence of the presence of ASR gel, particularly for the top and mid-



(a) Section 1: High severity cracks.  
Pavement constructed in 1960's



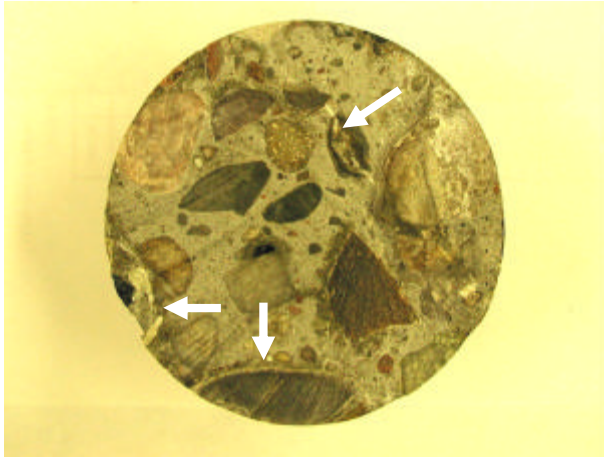
(b) Section 2: High severity cracks in  
pavement constructed in 1985; pavement  
condition is shown in the Figure 1 (a).



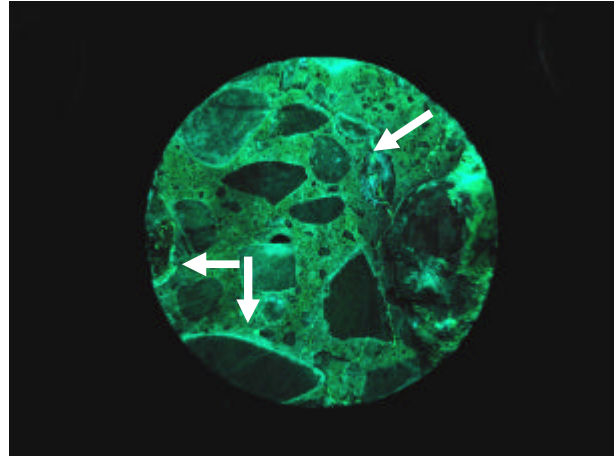
(c) Section 6: Low severity cracks in  
pavement constructed in 1987; pavement  
condition is shown in the Figure 1 (b).

**Figure 3.** Concrete cores collected from test sections showing cracks of varying severity

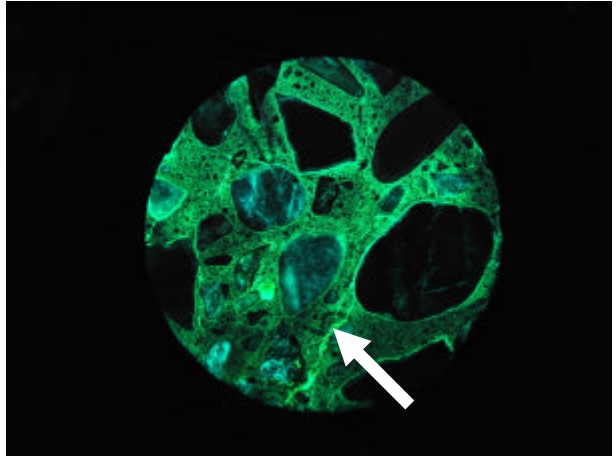
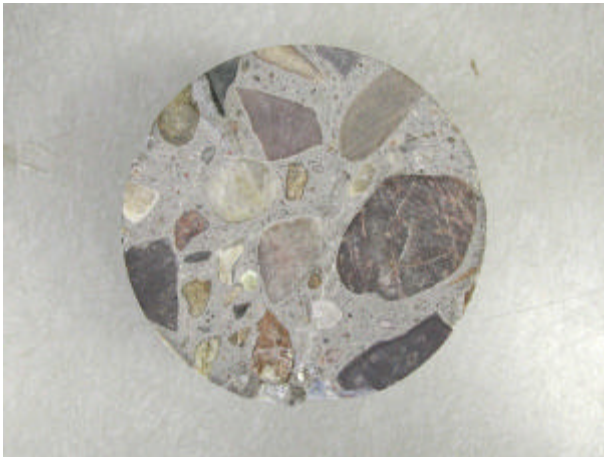
Under Ordinary Light



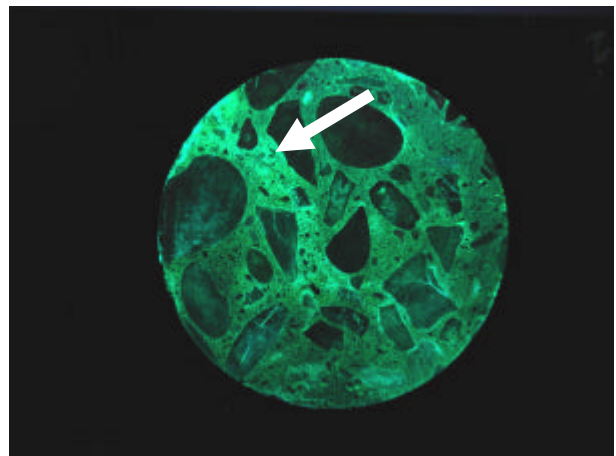
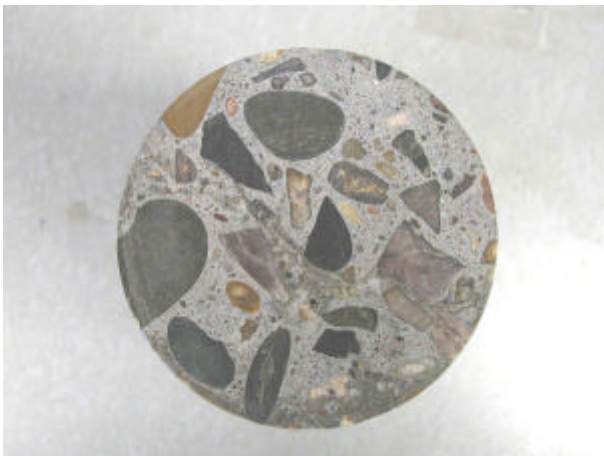
Under UV Light



(a) Cross-section at 2-inch depth



(c) Cross-section at 6-inch depth



(e) Cross-section at 12" depth (2.5-inch from bottom)

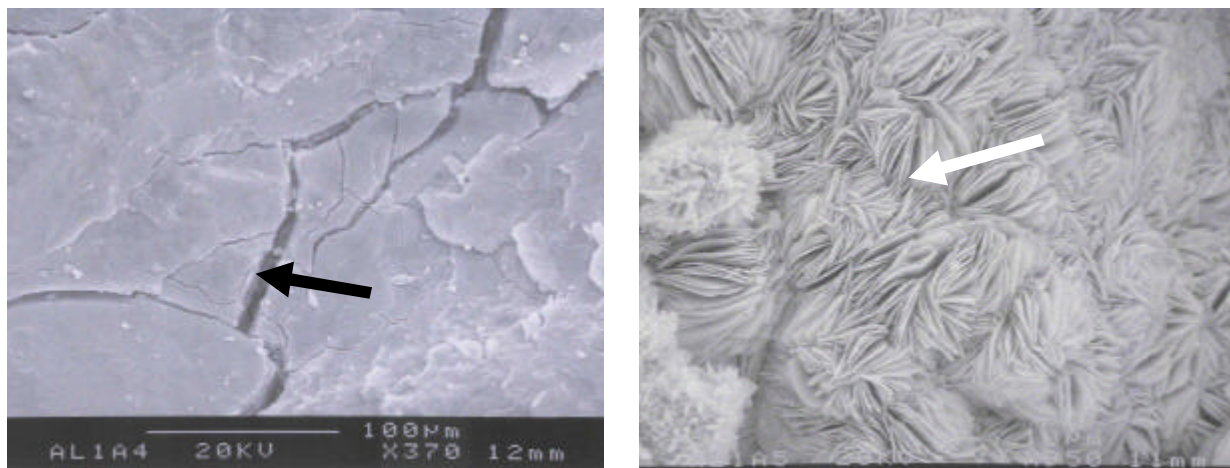
**Figure 4.** Laboratory application of UAFM to sliced core samples at different depths: The core was collected from test section 1 where the pavement surface showed severe map cracking that appeared through the seal coated surface.

depth samples. Although the bottom sample also displayed marginal amount of glow around aggregate particles, it was not a definitive identification of ASR compared to the upper samples. Nonetheless, this observation supports that ASR deterioration proceeds from upper surface to bottom of pavement slab.

UAFM was found to be effective for identification of ASR gel in the laboratory. According to the authors, in-field application of UAFM did not provide very satisfactory results. It is recommended that laboratory examination of core samples must be included in the framework of ASR distress evaluation. There are indications that the gel may exist without any expansion and subsequent deterioration. Therefore, other factors, such as moisture accessibility and environmental condition of the area, must be considered in addition to a detailed visual inspection of core samples before drawing conclusions about the distress under investigation, whether it has been caused by ASR, and if so, the extent of damage it has caused.

### Scanning Electron Microscopy/Energy Dispersive X-Ray Analysis (SEM/EDXA)

Microstructural analysis conducted on sliced core samples from section 1 is shown in the Figures 4 (a) and (c). Selected samples were taken from locations that previously displayed a bright glow by UAFM, and analyzed using SEM/EDXA. According to the analysis, the gel was noted to exist at paste-aggregate interface and also in the paste. Two types of gel morphology, namely the rosette type and the massive cracked type<sup>(5)</sup> of gel were observed in the paste. These are illustrated in Figure 5. Additionally, presence of lamellar gel was observed at the paste-aggregate interface (Figure 6). No difference in chemical composition was detected between the different types. Generally, the gel has a characteristic composition shown in Figure 7. Several air voids were packed with ettringite needles (Figure 8), but no signs of deterioration were observed around them. This implies that the main cause of distress in this pavement section is ASR. The C-S-H at times was found to be rich in potassium (Figure 9), whereas elsewhere only nominal amounts of impurities such as iron and aluminum were present (Figure 10).



(a) Massive gel

(b) Rosette-like gel

**Figure 5.** SEM images of ASR gel products in test sample from section 1

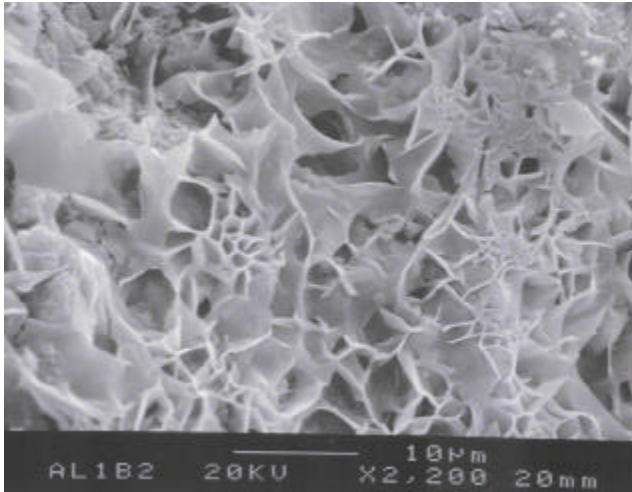


**Figure 6.** Lamellar gel at the surface of aggregate

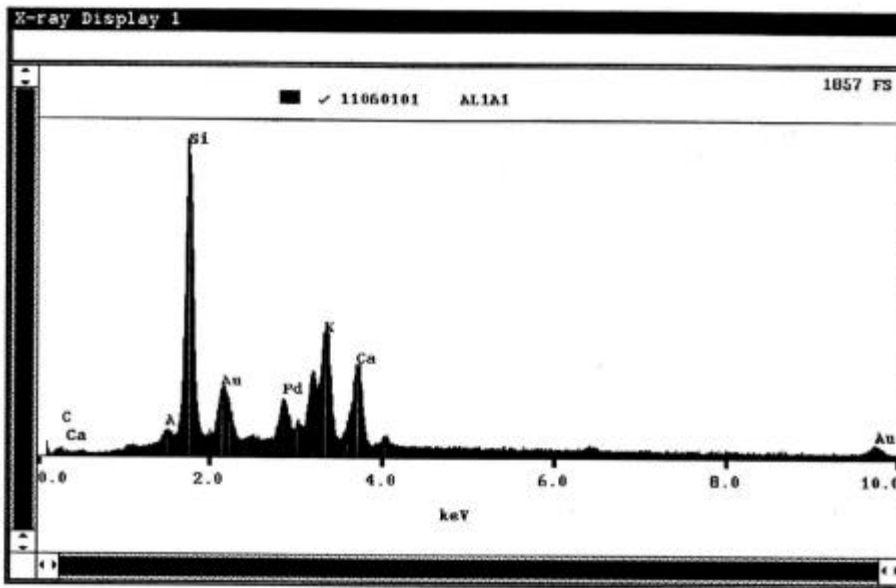


**Figure 7.** Composition of ASR gel (Ca, Si, K)

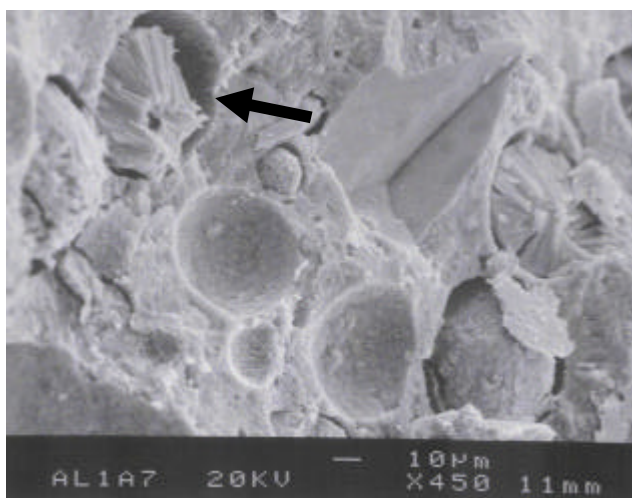


**Figure 8.** Ettringite formation in air voids: no signs of deterioration around the ettringite suggest ASR as a main cause of distress

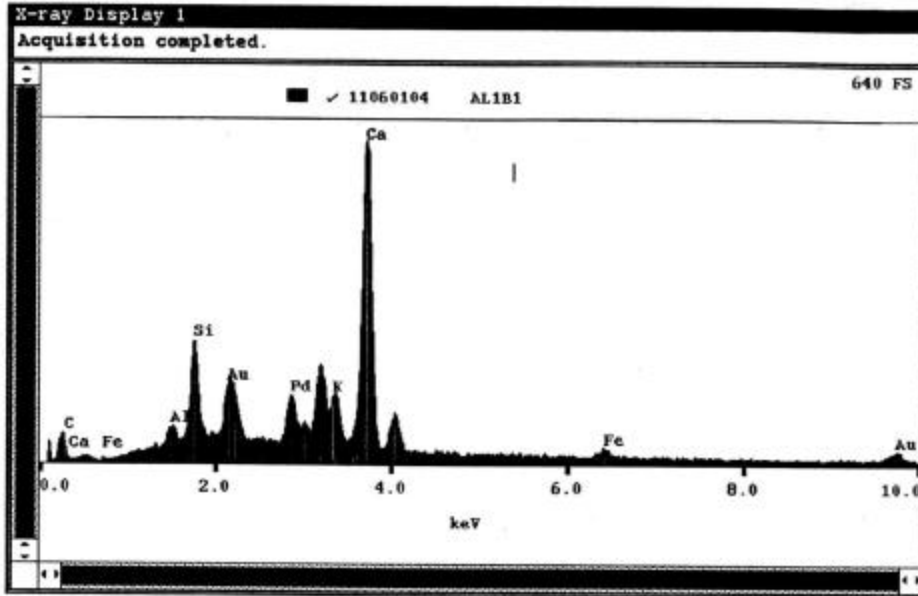


Figure 9. EDX spectrum of C-S-H showing high amount of potassium

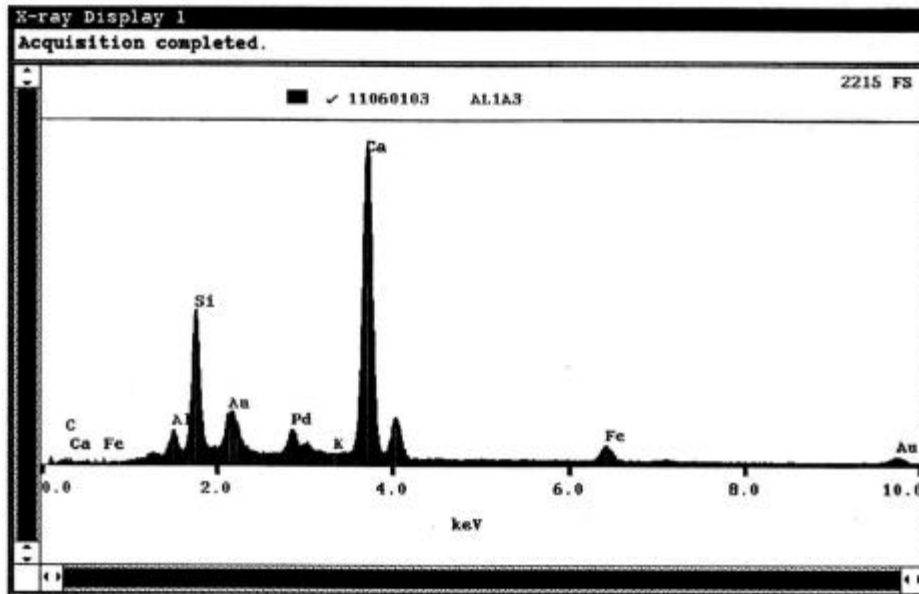


Figure 10. EDX of C-S-H showing only small amounts of Fe and Al as impurities

## CONCLUDING REMARKS

Distress features in airfield pavements including runway, taxiway, and aprons were evaluated for ASR distress. A framework was tentatively prepared to investigate distress type and extent in airfield pavements, consisting of runways, taxiways and aprons. The protocol consists of a detailed visual inspection, in-field detection of ASR gel, and laboratory investigation of core samples.

Besides field inspection, it is recommended to conduct laboratory analysis for more definite identification of ASR. UAFM was found to be an effective tool for the identification of ASR gel in the laboratory, but did not provide very satisfactory in-field application results. In addition to the examination of distress features, factors such as moisture accessibility and environmental condition of the area must be considered before drawing definite conclusions about the distress mechanism, whether it has been caused by ASR, and if so, the extent of damage resulting from it.

## ACKNOWLEDGEMENTS

This study is supported by the National Safe Skies Alliance. Funding was provided by the Federal Aviation Authority (FAA). The authors wish to thank the airport authorities for their special assistance during the fieldwork, and to Mr. Mike Provine, P.E. of Molzen-Corbin & Associates, and Mr. W.L. Bill Barringer, P.E., FACI, for their support.

## REFERENCES

1. D. Stark, *Handbook for the Identification of Alkali-Silica Reactivity in Highway Structures*, SHRP-C-315, Strategic Highway Research Program, National Research Council, Washington D.C., 1991.
2. M. Regourd, Product of Reaction and Petrographic Examination, *Proceedings, 8<sup>th</sup> International Conference on Alkali-Aggregate Reaction in Concrete*, Kyoto, Japan, 1989, pp.445-456.
3. G. E. Blight, J. R. McIver, W. K. Schutte, and R. Rimmer, The Effect of Alkali Aggregate Reaction on Reinforced Concrete Structures Made with Witwatersland Quartzite Aggregate, *Proceedings, 5<sup>th</sup> International Conference on Alkali-Aggregate Reaction in Concrete*, Cape Town, South Africa, 1981.
4. S. Diamond, ASR-Another Look at Mechanisms, *Proceedings, 8<sup>th</sup> International Conference on Alkali-Aggregate Reaction in Concrete*, Kyoto, Japan, 1989, pp.83-94.
5. M. Regourd and H. Hornain, Microstructure of Reaction Products, *Concrete Alkali-Aggregate Reactions, Proceedings, 7<sup>th</sup> International Conference on Alkali-Aggregate Reaction in Concrete, Ottawa, 1986*, Noyes Publication, 1987, pp.375-380.